Influence of dry-etching damage on the electrical properties of an AlGaN/GaN Schottky barrier diode with recessed anode*

Zhong Jian(钟 健)[a)], Yao Yao(姚 尧)[a)], Zheng Yue(郑 越)[a)], Yang Fan(杨 帆)[a)], Ni Yi-Qiang(倪毅强)[a)], He Zhi-Yuan(贺致远)[a)], Shen Zhen(沈 震)[a)], Zhou Gui-Lin(周桂林)[a)], Zhou De-Qiu(周德秋)[a)], Wu Zhi-Sheng(吴志盛)[a)], Zhang Bai-Jun(张伯君)[b)], and Liu Yang(刘 扬)[a)†]

[a)] *School of Physics and Engineering, Institute of Power Electronics and Control Technology, Sun Yat-Sen University, Guangzhou* 510275, *China*
[b)] *State Key Laboratory of Optoelectronic Materials and Technologies, Sun Yat-Sen University, Guangzhou* 510275, *China*

(Received 3 March 2015; revised manuscript received 13 April 2015; published online 20 July 2015)

The influences of dry-etching damage on the electrical properties of an AlGaN/GaN Schottky barrier diode with ICP-recessed anode was investigated for the first time. It was found that the turn-on voltage is decreased with the increase of dry-etching power. Furthermore, the leakage currents in the reverse bias region above pinch-off voltage rise as radio frequency (RF) power increases, while below pinch-off voltage, leakage currents tend to be independent of RF power. Based on detailed current–voltage–temperature (I–V–T) measurements, the barrier height of thermionic-field emission (TFE) from GaN is lowered as RF power increases, which results in early conduction. The increase of leakage current can be explained by Frenkel–Poole (FP) emission that higher dry-etching damage in the sidewall leads to the higher tunneling current, while below pinch-off voltage, the leakage is only related to the AlGaN surface, which is independent of RF power.

Keywords: AlGaN/GaN Schottky barrier diodes, recessed anode, etching damage, tunneling

PACS: 73.30.+y, 81.05.Ea, 73.40.Kp **DOI:** 10.1088/1674-1056/24/9/097303

1. Introduction

GaN is known as an attractive material for semiconductor power devices due to high breakdown field, high saturation drift velocity, and good thermal properties. Owing to the high sheet carrier concentration in two-dimensional electron gas (2DEG),[1,2] AlGaN/GaN heterostructure Schottky barrier diode (SBD) is widely used in high-power-switching applications. However, conventional planar AlGaN/GaN SBDs exhibit an undesired high onset voltage (V_{on}), which leads to significant conduction loss in switching condition. Various AlGaN/GaN SBDs employing a dual Schottky anode or field effect structure have been proposed to reduce V_{on}.[3–6] Recently, a new AlGaN/GaN SBD structure was proposed with a fully recessed anode and Schottky metal directly contacting the 2DEG,[7,8] which has drawn much attention because of its capacity to reduce the onset voltage without sacrificing the low leakage current. Previous study has investigated the current transport mechanism of the recessed SBD, which indicated that the recessed-anode sidewall is important to the electrical properties in both forward and reverse biases.[9] In particular, dry-etching damage on the sidewall induced during the anode-recessed dry-etching process could drastically affect the electrical properties. Thus in order to further improve the device performance, it is necessary to clarify the influence of dry-etching damage on electrical properties during the anode recessing process. Among all the parameters of the etching process, RF power provides the collision energy for plasma and has a critical influence on the roughness of etched GaN.[10] In this paper, we report etching results as a function of RF power.

In this study, AlGaN/GaN SBDs with a recessed-anode of different dry-etching power were fabricated to investigate the influence of dry-etching damage on the electrical properties for the first time. Detailed current–voltage–temperature (I–V–T) measurements were performed to give insight of forward and reverse current–voltage characteristics over the range of 298 K $< T <$ 473 K. Conduction properties of the AlGaN/GaN surface were also evaluated by conductive atomic forced microscopy.

2. Experiment

The cross-section view and the fabricated image of the recessed AlGaN/GaN SBDs are shown in Fig. 1. AlGaN/GaN heretostructures were grown by metal organic chemical vapor deposition (MOCVD) on a 2-inch Si (111) substrate. The epilayer consisted of a 20-nm high-temperature AlN (HT-AlN, $\sim$ 1000 °C), followed by a 1.4-μm undoped semi-insulating GaN (Si-GaN) layer with two 15-nm low-temperature AlN

*Project supported by the National Natural Science Foundation of China (Grant Nos. 51177175 and 61274039), the National Basic Research Program of China (Grant Nos. 2010CB923200 and 2011CB301903), the Ph. D. Programs Foundation of Ministry of Education of China (Grant No. 20110171110021), the International Science and Technology Collaboration Program of China (Grant No. 2012DFG52260), the National High Technology Research and Development Program of China (Grant No. 2014AA032606), the Science and Technology Plan of Guangdong Province, China (Grant No. 2013B010401013), and the Opened Fund of the State Key Laboratory on Integrated Optoelectronics, China (Grant No. IOSKL2014KF17).

†Corresponding author. E-mail: liuy69@mail.sysu.edu.cn

© 2015 Chinese Physical Society and IOP Publishing Ltd

(LT-AlN, ∼ 700 °C) interlayers, and a 25-nm AlGaN barrier layer with a nominal 30% Al composition. A sheet carrier density of 1×10^{13} cm^{-2} and an electron mobility of ∼ 1200 cm^2·V^{-1}·s^{-1} were determined by room-temperature Hall measurements.

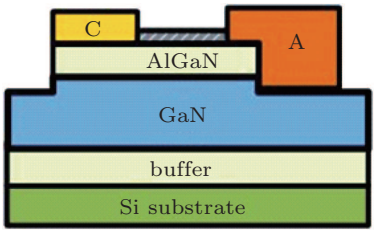


Fig. 1. (color online) Cross-section view of the AlGaN/GaN heterojunction SBD with fully recessed SBD.

Device isolation and anode recessing were accomplished by BCl_3/Cl_2 inductively coupled plasma (ICP) etching simultaneously. For the comparative study, ICP powers were set as 300 W and RF bias powers were set over a range of 10 W–80 W. Based on the scanning electron microscope (SEM) in Fig. 2, steep sidewalls were observed after the etching process except in that at 80 W, which formed large particles on the sidewall. Ti/Al/Ni/Au (15/80/25/80)-based cathode was then fabricated on the wafer and annealed at 870 °C for 30 s in ambient nitrogen. The AlGaN layer was passivated with 300-nm SiO_2 prepared by plasma-enhanced chemical vapor deposition (PECVD) at 350 °C. A trench for the anode Schottky was defined in the passivation layer by lithography and subsequent wet etching by buffered hydrofluoric acid. Ni/Au (25/60 nm) was formed on the surface as well as the sidewall by electron-beam evaporation. Thus the anode contained a Ni/Au-AlGaN contact on the planar surface with 3-μm length and a Ni/Au-GaN contact directly contacting the 2DEG with a thinner barrier. The distance between an anode and a cathode was 20 μm and the electrode width was 100 μm. Electrical properties were characterized by the current–voltage (I–V) measurement and current–voltage–temperature measurements (I–V–T) using Agilent 1505A.

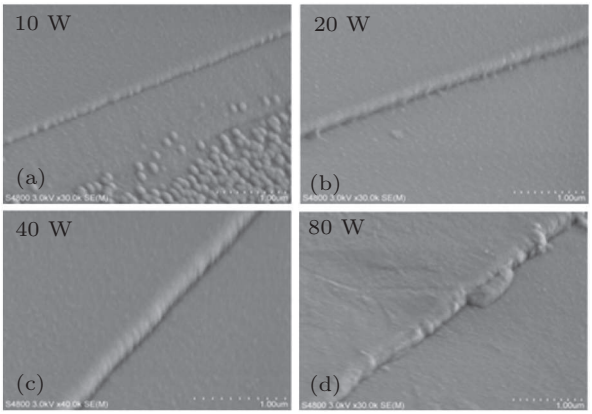


Fig. 2. SEM view of recessed SBD dry-etching sidewall morphology with RF bias powers of 10 W (a), 20 W (b), 40 W (c), and 80 W (d).

3. Result and discussion

Typical current–voltage characteristics were measured to clarify the influence of dry-etching damage on the electrical properties for the recessed SBD. Figure 3 shows the typical experimental forward and reverse I–V characteristics of recessed SBD with L_{ac} of 30 μm, V_{on} is defined as the voltage-axis intercept of the forward I–V curves in the linear region. To clarify the relationship between turn-on voltage and etching power, the plot of V_{on} as a function of the recessed-anode etching power is shown in Fig. 4. It is clear that V_{on} of the recessed SBD is lowered with the increase of RF power from 10 W to 80 W. A distinct reduction of V_{on} as the etching power increases is observed. In the reverse bias, the leakage current shows two different behaviors above and below pinch-off voltage. In the reverse bias above pinch-off voltage, an increase of leakage current is observed when the etching power increases.

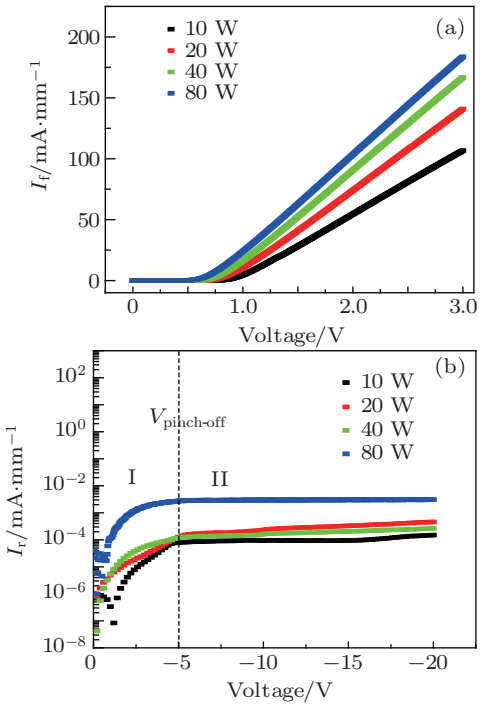


Fig. 3. (color online) Typical experimental forward (a) and reverse (b) I–V characteristics of recessed-SBDs. Here, region I: $0 > V > V_{pinch-off}$, region II: $V < V_{pinch-off}$.

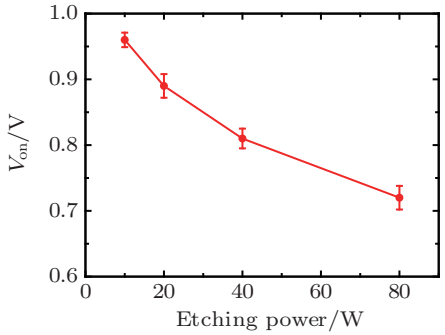


Fig. 4. (color online) The V_{on} of recessed-SBDs as a function of the RF etching power.

However, when the reverse bias drops below the pinch-off voltage, leakage current saturates and I_r (reverse current) of samples with etching power from 10 W to 40 W remains in the same magnitude of 1×10^{-4} mA/mm. It indicates that leakage current below pinch-off voltage is independent of the etching power. Note that an exception of samples of 80-W etching power with leakage current of 1×10^{-2} mA/mm is observed as well. It is believed that the etching process with excessive etching power causes significant damage to the bulk material. The behaviors above suggest that increasing etching power in an appropriate range contributes to the reduction of the turn-on voltage without sacrificing the low leakage current of the recessed SBDs. This phenomenon has not been reported previously.

In order to give insight into the influence of dry-etching damage on the electrical properties above, current–voltage–temperature (I–V–T) measurements were performed over a range of 298 K$< T <$ 473 K. In the forward bias, we took account of a tunneling transport component based on the thermionic-field emission (TFE) model to fit the experiment curves. A previous study has reported that TFE is the dominant current transport mechanism for the recessed AlGaN/GaN SBD.[9] Under the forward bias, the current due to TFE is given by[11,12]

$$J_{\rm TFE} = \frac{A^*T\sqrt{\pi E_{00}q(\phi_{\rm Bn}-\phi_{\rm n}-V_{\rm F})}}{k\cosh(E_{00}/kT)} \times \exp\left[\frac{-q\phi_{\rm n}}{kT}-\frac{q(\phi_{\rm Bn}-\phi_{\rm B})}{E_0}\right]\exp\left(\frac{qV_{\rm F}}{E_0}\right), \quad (1)$$

with

$$E_0 \equiv E_{00}\coth\left(\frac{E_{00}}{kT}\right), \quad (2)$$

$$E_{00} \equiv \frac{q\hbar}{2}\sqrt{\frac{N}{m^*\varepsilon_0\varepsilon_{\rm s}}}, \quad (3)$$

where A^* is the Richardson constant, T is the absolute temperature, $\phi_{\rm Bn}$ is the Schottky barrier height (SBH), $\phi_{\rm n} = (E_{\rm C} - E_F)/q$, k is the Boltzmann constant, and E_{00} represents the tunneling characteristic energy. Here, $\phi_{\rm Bn}$ and N are taken as the fitting variables to fit in the experiment curves. Figure 5 shows the forward I–V–T curves of recessed AlGaN/GaN SBD and calculated I–V–T curves by the TFE model. The linear portion of the measured curves is fitted well to the calculated curves with N and $\phi_{\rm Bn}$ in a wide range of temperature from 298 K to 473 K. To illuminate the relationship of calculated concentration N and barrier height $\phi_{\rm Bn}$ to the RF power, a plot of N and $\phi_{\rm Bn}$ as a function of RF power is shown in Fig. 6. It is clear that the equivalent Schottky barrier height decreases with the increase of dry-etching power. The reduction of $\phi_{\rm Bn}$ is consistent with the reduction of $V_{\rm on}$. Moreover, doping concentration N of SBD was calculated as 4×10^{18} cm^{-3}, 4×10^{18} cm^{-3}, 4.5×10^{18} cm^{-3}, and 6×10^{18} cm^{-3} for recessed-SBD with etching power of 10 W, 20 W, 40 W, and 80 W respectively. Note that the doping concentration N becomes larger as the ICP etching power increases. The calculated concentration is approximately the same magnitude as that of 2DEG. Therefore, the equivalent

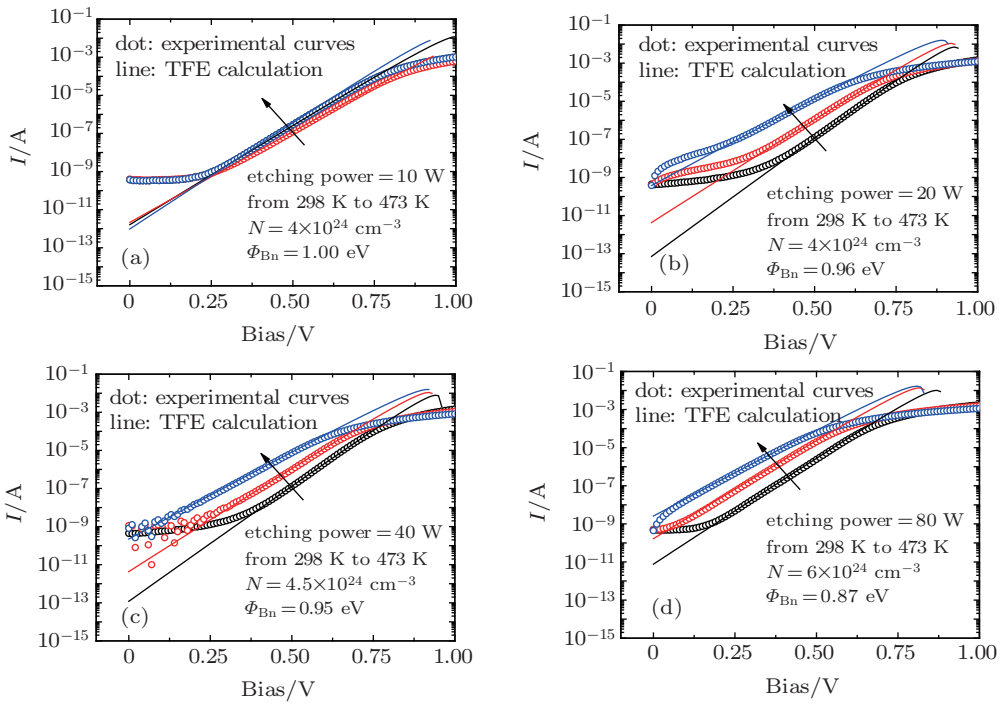


Fig. 5. (color online) I–V–T curves of recessed AlGaN/GaN SBD in the forward bias region and calculated I–V–T curves by the TFE model. (a) Etching power = 10 W, $N = 4\times10^{24}$ cm^{-3}, $\phi_{\rm Bn} = 1.00$ eV; (b) etching power = 20 W, $N = 4\times10^{24}$ cm^{-3}, $\phi_{\rm Bn} = 0.96$ eV; (c) etching power = 40 W, $N = 4.5\times10^{24}$ cm^{-3}, $\phi_{\rm Bn} = 0.95$ eV; (d) etching power = 80 W, $N = 6\times10^{24}$ cm^{-3}, $\phi_{\rm Bn} = 0.87$ eV.

doping concentration N is related to the concentration of 2DEG channel. The increase of N suggests that the dry-etching process with high RF power induces additional donor-like defects, which contributes to the increase of concentration of the conductive channel. The higher the etching power in the process, the more defects will be induced to the channel. A recent theoretical study has proposed that the ICP etching process produces N vacancies (V_N),[13,14] which behave as donor states near the conduction band edge. As the dry-etching power increases, the ICP-etched surface including the sidewall becomes more N-deficient and produces V_N-related defects. These defects and/or their complex may provide a conducting path with a lower barrier, which increases the tunneling probability for the thermally excited electrons. The lateral conducting path is conducted with lower V_{on}. This explains the reason for the early conduction and reduction of V_{on}.

To understand the influence of dry-etching damage on reverse leakage, current–voltage–temperature measurement was further performed in the reverse leakage bias. As discussed, reverse current transport through different paths when the reverse bias is above or below pinch-off voltage. Therefore, two different mechanisms are discussed separately.

(i) In the reverse bias above pinch-off voltage, the 2DEG channel under Schottky metal is not depleted completely. The reverse current path consists of the surface Ni/Au-AlGaN contact and the sidewall Ni/Au-GaN contact. The leakage current is codetermined by FP emission on the AlGaN surface and tunneling on the sidewall. To investigate the effects of the dry-etching power damage, the reverse experimental curves were fitted by Frenkel–Poole emission model. The current density calculated as the FP model is given by

$$J_{\mathrm{FP}} = CE_{\mathrm{b}} \exp\left[-\frac{q(\phi_t - \sqrt{qE_{\mathrm{b}}/\pi\varepsilon_0\varepsilon_{\mathrm{s}}})}{kT}\right], \tag{4}$$

where E_{b} is the electric field in the semiconductor barrier at the M–S interface and is assumed to be constant within the AlGaN barrier layer, ϕ_{t} is the barrier height for electron emission from the trapped state, ε_{s} is the relative dielectric permittivity at high frequency, T is the absolute temperature, and k is Boltzmann constant. In Eq. (4), the current transport equation can be rearranged as

$$\ln(J_{\mathrm{FP}}/E_{\mathrm{b}}) = m(T)\sqrt{E_{\mathrm{b}}} + b(T), \tag{5}$$

where

$$b(T) = -\frac{q\phi_t}{kT} + \ln C. \tag{6}$$

As shown in Fig. 7(a) (only 20 W is given), the current $\ln(J/E)$ versus $\sqrt{E}$ plots of the measured reverse bias current density above pinch-off voltage ($-5\ \mathrm{V} < V < 0\ \mathrm{V}$) are well described by the electric-field dependence of Eq. (5). Figure 7(b) shows the function of calculated ϕ_{t} versus etching power of the ICP process based on the calculation of Eq. (6) from the slope of $b(T)$ versus $1/T$ plots. The data points fit well with straight lines. Note that the calculated ϕ_{t} is lowered as the etching power becomes higher. This trend may be due to the increasing recessed-sidewall tunneling currents. FP emission refers to electric-field-enhanced thermal emission from a trapped state into a continuum of electron states,[15] where ϕ_{t} represents the emission barrier height for the trapped states. It can be concluded that the barrier height for the FP emission is lowered as the RF power becomes higher. When the RF power becomes higher, more traps are induced on the sidewall, which increase the tunneling probability for the lateral conduction path. Therefore, the total leakage current increases with the sidewall tunneling current.

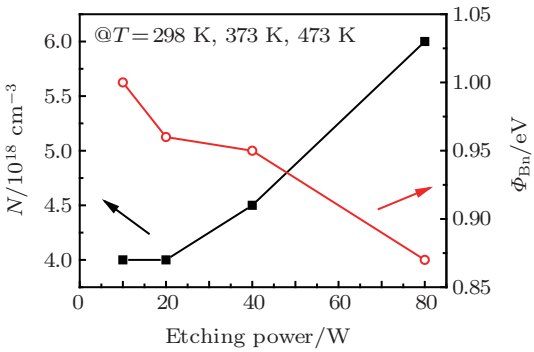


Fig. 6. (color online) Calculated concentration N and barrier height ϕ_{Bn} as a function of ICP RF power.

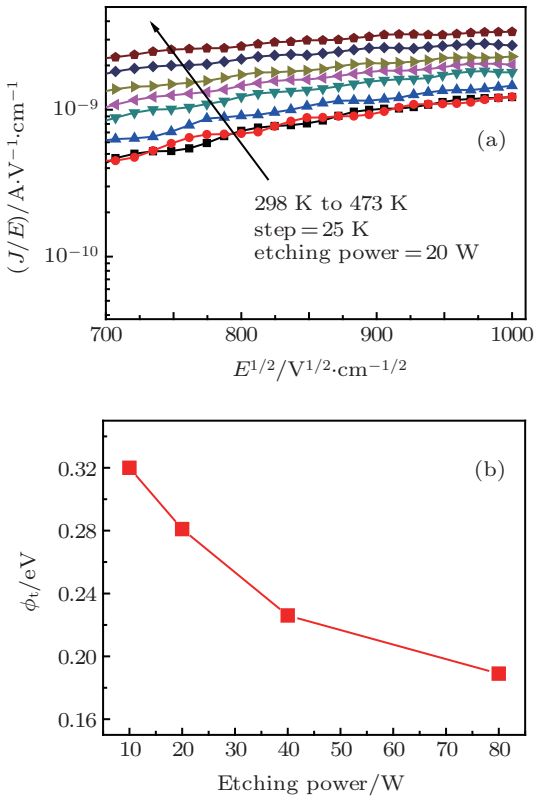


Fig. 7. (color online) (a) Leakage current density divided by electric field versus square root of electric field for Schottky contact of recessed SBD. (b) The plots of calculated ϕ_{t} versus etching power of the ICP process.

(ii) In the reverse bias below the pinch-off voltage ($V < -5$ V), the 2DEG channel is completely blocked. The leakage current saturates and mainly transports through the vertical Schottky contact. The leakage current is only related to the trap concentration of the planar AlGaN surface, which is protected by photoresist during the etching process. As the surface is independent of the RF power, the leakage current should saturate in the same magnitude regardless of the change of RF power. However, in the condition of excessive RF power of 80 W, the device shows an undesired high leakage current. That is mainly due to the AlGaN surface damage induced by excessive RF power. Figure 8 shows conductive atomic-forced microscope (CAFM) scan pictures of AlGaN surfaces for SBDs. For the sample of 80 W, large quantities of leakage peaks appear on the AlGaN surface. As the mesa surface is protected by photoresist, it indicates that the etching process with excessive RF power would penetrate through the photoresist and cause significant damage to the AlGaN surface. Therefore, an appropriate RF power should be considered without any damage induced to the AlGaN surface.

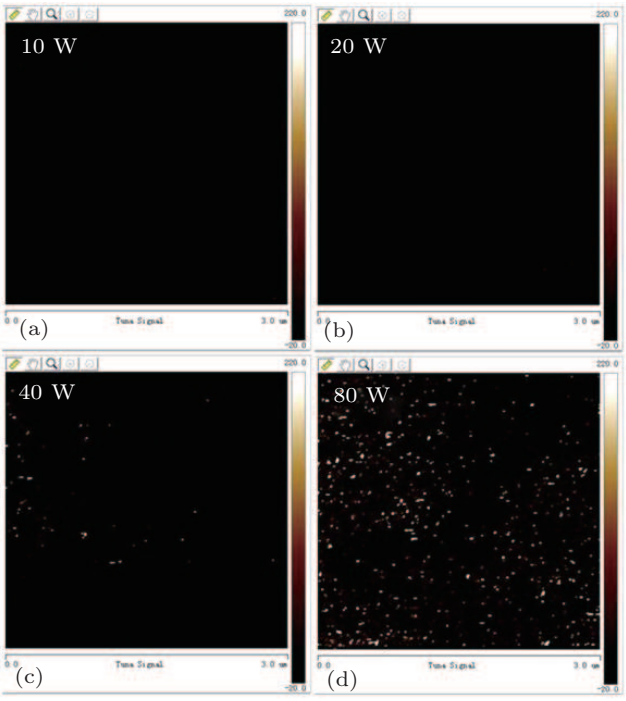


Fig. 8. (color online) CAFM photographs with etching powers of 10 W (a), 20 W (b), 40 W (c), and 80 W (d).

According to the electrical properties and the I–V–T analysis above, the influence of the dry-etching damage can be explained as follows. Reductions of V_{on} with the increase of RF power can be explained by TFE model. As the RF power increases, more defects are induced on the sidewall during the etching process, which increase the tunneling probability and result in early conduction. In the reverse bias above pinch-off voltage, the 2DEG channel under Schottky metal is not depleted completely and sidewall tunneling contributes to the total leakage current as calculated by the FP model. When the reverse bias is below the pinch-off voltage, the 2DEG channel is completely blocked and the leakage current is mainly transported through the vertical Schottky contact. However, when the excessive RF power is applied, the etching process would affect the AlGaN surface and cause the increase of the leakage current.

4. Conclusion

Influences of dry-etching damage on the electrical properties of an AlGaN/GaN Schottky barrier diode with a recessed anode was investigated for the first time. Reduction of V_{on} with the increase of RF power was observed in the forward bias. Leakage current increases as the RF power rises above the reverse bias above the pinch-off voltage. When the reverse bias is below the pinch-off voltage, leakage current saturates in the same magnitude. By increasing RF power in an appropriate range during the dry-etching process, the turn-on voltage of recessed SBDs can be reduced without the increase of leakage current. As calculated by the TFE model, the barrier height of thermionic-field emission (TFE) from GaN is lowered as RF power increases, which results in early conduction. The increase of doping concentration indicates that the dry-etching process induces donor-type defects, which increase the tunneling probability on the sidewall. In the reverse bias region above the pinch-off voltage, the higher ICP etching power increases the density of defects to lower the barrier height for FP emission. Below the pinch-off voltage, the leakage current is only related to the AlGaN surface and saturates in the same magnitude in an RF power range of 10 W–40 W. When the RF power is excessive, the AlGaN surface is damaged and the leakage current rises.

References

[1] Jiang C, Lu H, Chen D J, Ren F F, Zhang R and Zheng Y D 2014 *Chin. Phys. B* **23** 97308
[2] Tang C, Xie G, Zhang L, Guo Q, Wang T and Sheng K 2013 *Chin. Phys. B* **22** 106107
[3] Chen W, Wong K Y, Huang W and Chen K J 2008 *Appl. Phys. Lett.* **92** 253501
[4] Yoshida S, Li J, Ikeda N and Hataya K 2005 *Phys. Status Solidi C* **2** 2602
[5] Wang Z G, Chen W J, Zhang B and Li Z J 2012 *Chin. Phys. Lett.* **29** 107202
[6] Tokuda H, Watanabe F, Syahiman A, Kuzuhara M and Fujiwara T 2011 *IWPT* **2**
[7] Ha M W, Lee S C, Choi Y H, Kim S S, Yun C M and Han M K 2006 *Superlattices Microstruct.* **40** 567
[8] Treidel E B, Hilt O, Wentzel A, Wuerfl J and Traenkle G 2013 *Physica Status Solidi C* **10** 849
[9] Yao Y, Zhong J and Zheng Y 2015 *Jpn. J. Appl. Phys.* **54** 011001
[10] Shul R, McClellan G B and Casalnuovo D J 1996 *Appl. Phys. Lett.* **69** 1119
[11] Hashizume T, Kotani J and Hasegawa H 2004 *Appl. Phys. Lett.* **84** 4884
[12] Kotani J, Hasegawa H and Hashizume T 2004 *Appl. Surf. Sci.* **237** 213
[13] Choi K J, Jang H W and Lee J L 2003 *Appl. Phys. Lett.* **82** 1233
[14] Lan W H, Huang K C and Huang K F 2006 *Solid-State Electron.* **50** 1677
[15] Zhang H, Miller E J and Yu E T 2006 *J. Appl. Phys.* **99** 023703